PAPER • **OPEN ACCESS**

Preparation and characterization of metal mine tailings based backfiling material through geopolymerization

To cite this article: J Xing *et al* 2019 *IOP Conf. Ser.: Mater. Sci. Eng.* **479** 012023

Preparation and characterization of metal mine tailings based backfiling material through geopolymerization

J Xing, Y L Zhao, Q Wang[1], J P Qiu and X G Sun

College of Resources and Civil Engineering, Northeastern University, Shenyang, 110819, China;

[1] E-mail: 1601437@stu.neu.edu.cn

Abstract. The main objective of this study was to investigate the potential of using metal mine tailings (MT) as raw material for backfilling material preparation through geopolymerization. Due to the low reactivity of this aluminosilicate material in alkali solution, MT was pretreated through alkali fusion with various amounts of NaOH at 550℃ for 30min. XRD, FTIR and ICP-OCE testing results showed that the reactivity of MT was improved by alkali fusion pre-treatment. Different paste backfilling material (BFM) samples were prepared by adding water to the fused mine tailings (FMT). Compressive strength testing of BFM samples showed that, adding 20% NaOH during alkali fusion could satisfy the requirement of backing filling. As a result, by enhancing the reactivity of MT through alkali fusion pretreatment, MT can be recycled as an alternative raw material to be used as the replacement of Portland cement for mine filling.

1. Introduction

Mining industries worldwide generate massive tailings after valuable metals and minerals separation from ore [1]. It has been reported that the volume of mine tailings generated is about 97-99% of total ore processed [2]. Most of mine tailings are stockpiled in tailings dams because there has not been a plant scale application for the utilization of this waste materials. The disposal of mine tailings often require large land areas to be used as tailings wasteland leading to invasion on agricultural land [3, 4]. Other challenges concerning mine tailings treatment include high disposal cost and latent leaching of toxic elements such as Pb, Cd and beneficiation reagent from the tailings into surrounding soil or ground water [5, 6], threatening human's health. Also, tailings ponds are major hazard sources that may result in geological disasters such as landslide and debris flow [4, 7, 8]. Therefore, it is of great importance to optimize the utilization of mine tailings and subsequently minimize environmental influence.

Recovery of valuable residual elements such as Au, Ag, Zn and Cu from mine tailings has been ever reported [9-11]. However, the cost of recovery process is high and a large amount of residues after the extraction still need disposal. Other attempts to the utilization of mine tailings into materials have also been reported. Pia et al. [12] have studied the use gold tailings as art pottery body material. The pottery body made of gold tailings met the performance requirements of art pottery body because of their close-grind inner structure. Yilmaz et al. [13] have explored the suitability to prepare ordered mesoporous silica SBA-15 from gold tailings. The results shown that only the weight ratio of NaOH /slurry influenced S_{BET} (specific surface area) significantly. Onuaguluchi et al. [14] explored the effects of copper tailings on the reinforcement corrosion initiation time and deterioration in copper

tailings blended concrete. Results showed that delayed corrosion initiation was observed in all samples containing copper tailings as an additive. Despite many efforts towards exploitation of mine tailings, the commercial application is limited due to concerns about its leachability and consequent environment implications.

Another solution for consuming these huge amounts of mine tailings is to utilize these substances as mining backfilling material. Backfilling involves placing any waste material in underground mined-out areas for the purpose of either disposal or engineering functions [15]. In the last decade, researches on backfilling material using industrial waste, such as fly ash and blast furnace slag, have been conducted [16], and have demonstrated their excellent workability and good mechanical properties [17, 18]. However, there are few reports on the utilization of metal mine tailings to prepare backfilling material through geopolymerization.

Geopolymer refers to inorganic materials prepared from the reaction of an alkali source with an aluminosilicate precursor [19, 20], which have shown potential to offer an environment friendly alternative to Portland cement, and are increasingly being used in various situations [21-25]. Although a wide variety of industrial by-products such as fly ash [26, 27], granulated blast furnace slag [28, 29], red mud [30] etc., have been reported to be synthesized into high performance materials for construction and building applications through geopolymerization, limit researches have been reported on the preparation of geopolymer using metal mine tailings [5, 25, 31] as raw material. It is probably because that metal mine tailings enjoy low degree of reactivity in alkali solution due to their mineralogical composition which generally comprise high crystallized minerals [32, 33]. Recently, alkali fusion treatment using to improve pozzolanic properties of raw materials before geopolymerization has been reported [34, 35]. The present study investigated the feasibility to prepare geopolymer using metal mine tailings (MT) as raw material. The effect of NaOH dosage was evaluated because the degree of alkaline fusion pretreatment may influence the properties of fused mine tailings (FMT) and FMT based backfilling material.

2. Materials and methods

2.1. Materials

MT was provided by Zhaojin Mining Industry Co., Ltd in Zhaoyuan, China. It was dried at 105°C for 24 hours. The chemical composition of MT was presented in Table 1, respectively. NaOH pellets of 99% purity were used as alkali source during fusion treatment.

Table 1. Chemical composition of MT (wt. %).

Components	SiO_2	Al_2O_3	MgO	CaO	Fe_2O_3	Na_2O	K_2O	SO_3
MT	69.55	12.63	0.33	0.69	0.87	1.98	3.13	0.68

2.2. Methods

2.2.1. Alkali fusion process. Dry MT was mixed with 10, 20, 30, 40 and 50% of NaOH with respect to the mass of MT and then ground in a planetary ball mill for 1 min to assure homogenous blending of the powders. The mixtures were then heated in an electric resistance furnace at 550 °C for 30 min at a heating rate of 10 °C/min before cooling naturally in the furnace to room temperature. After that, the fused MT were crushed and sieved at 74 μm. The fused mine tailings (FMT) containing 10, 20, 30, 40 and 50 % of NaOH with respect to the mass of MT were shown in Table 2.

Table 2. Mix proportions of FMT.

NaOH content/wt.%	10	20	30	40	50
FMT	FMT1	FMT2	FMT3	FMT4	FMT5

2.2.2. Backfilling material preparation. As for backfilling materials (BFM) samples preparation, water was added to the mixture of FMT (20 wt. %) and mine tailings (without fusion treatment) (80 wt. %) at a solid/liquid mass ratio of 3.5/1 and mixed in a mechanical mixer for 5 min. The resulting paste was molded, then vibrated for 3 min on an electric vibrating table to remove entrapped air bubbles. The molds were cured at ambient temperature until testing. As a control sample, MT was mixed with NaOH solution (10M) with the solid/liquid ratio of 3.5/1 and cured at the same condition. The BFM samples prepared from MT and FMTi will be mentioned as BFMi, i=0, 1, 2, 3, 4 and 5 thereafter.

2.2.3. Characterization. Thermal analysis of MT sample was performed using Diamond TG-DSC (Netzsch STA 409 PC/PG, German). The temperature was raised up from 25 to 1200°C at a heating rate of 10°C/min in an alumina crucible under N_2 atmosphere.

To determine the amount of reactivity content contained in MT and the FMT, the method performed by [36] was used. This method involves the treatment 3 g of sample with 30 ml of NaOH (10 mol/L) with constant stirring for 1 hour at 60°C and then filtered. Inductively Coupled Plasma optical emission spectroscopy (ICP-OES, Optima 8300DV, America) was used to determine the concentration of dissolved elements.

Microtopography was determined by scanning electron microscopic (SEM) using a Phillip XL 30 SEM (Phillips, Holland).

X-ray diffraction (XRD) patterns were obtained using an X'Pert Pro XRD (Philips, Holland) at a scanning rate of 0.1 deg s^{-1} in the 2θ range of 10 to 80°.

Fourier-transform infrared spectroscopy (FTIR) tests were performed by NEXUS 470 (America) with a wavelength of 4000-400 cm^{-1} to identify the functional group of the materials.

Compressive tests were conducted to study the ultimate strength of BFM samples. The tests were carried on samples after 28 days of curing. Data reported were the average of 3 samples.

3. Results and discussion

3.1. Characterization of MT and FMT

The XRD patterns of MT(metal mine tailings) and FMT(fused metal mine tailings) samples were shown in Figure 1. Mineralogical analysis of MT (Figure 1 a) showed highly crystallized structure, consisting of quartz, albite and trace of sodalite and muscovite. This is the main reason why MT are less used in the preparation of geopolymer. After calcined at 550℃, the XRD patterns of FMT samples showed that all the initial minerals contained in MT remained (but showed a significant decrease in peak intensities) except muscovite which was totally disappeared in the samples of FMT5. Tchakoute et al observed similar phenomena [37]. As Tchakoute et al. explained that muscovite is an aluminosilicate which can reacted with NaOH by geopolymerization reaction or be dissolved in fused NaOH [37]. Along with the decrease in peak intensities of initial minerals, a new crystalline phase (sodium silicate, Na_2SiO_3) was identified. The formation of Na_2SiO_3 phase results from the decomposition of initial aluminosilicate minerals (quartz, albite, sodalite and muscovite) during the calcination process liberating SiO_4 and combination with Na^+ from fused NaOH [36]. The NaOH alkali fusion reaction could be described as follows [38]:

$$Na_2O+Al_2O_3 \rightarrow 2NaAlO_2 \quad (1)$$

$$Na_2O+SiO_2 \rightarrow Na_2SiO_3 \quad (2)$$

$$2NaAlO_2+nNa_2SiO_3 \rightarrow Na_2O \cdot Al_2O_3 \cdot nSiO_2+nNa_2O \quad (3)$$

From Figure 1 b, c and d, an increase in the intensity of Na_2SiO_3 phase as a function of NaOH dosage was observed. This could be explained by the fact that the more free-Na^+ and higher alkalinity could promote the reaction in the alkali roasting system. This result was in agreement with the reports by Tchakoute et al. [37] and Tchadjié et al. [36] where the amount of an Na_2SiO_3 phase content was depending on Na_2O content or Al_2O_3/Na_2O molar ratio.

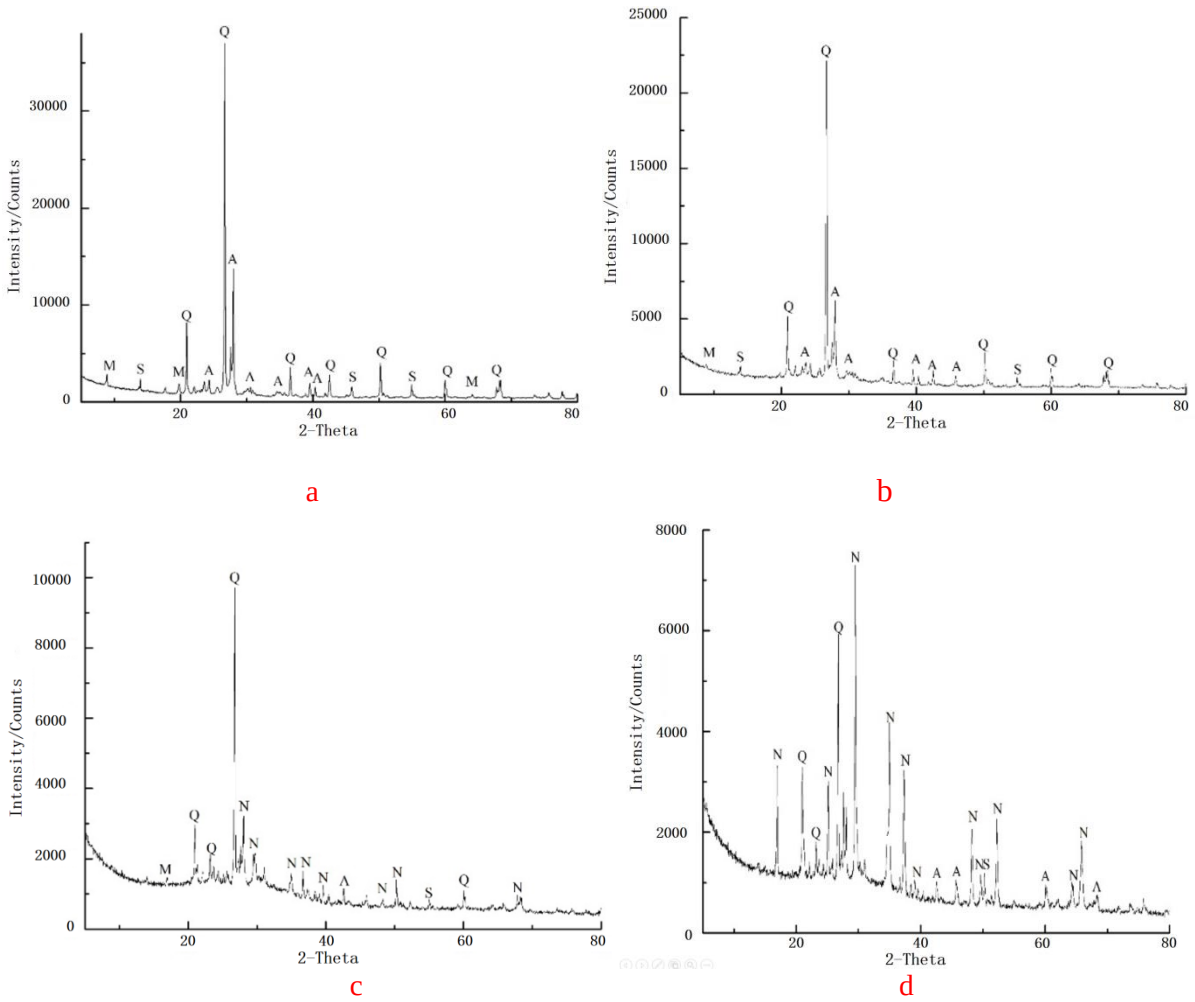

Figure 1. XRD patterns of MT (a) and FMT (b=FMT1; c=FMT3; d=FMT5). (Q-Quartz, A-Albite, S-Sodalite, M-Muscovite, N-Sodium Silicate).

The TG and DSC curves of the MT and FMT3 specimens were shown in Figure 2. From Figure 2 a, we could see that the total mass loss of MT sample was 8.8% from 20 to 1200 °C. This loss (1.2 %) which produced an endothermic peak at 212.4 °C was likely attributed to the physical water content of the MT sample. The small endothermic peak at 550-580 °C was result from the reversible β-α quartz transition [38]. In the presence of 30% NaOH (Figure 2 b), the weight loss of MT presented in the curve can be separated into four stages up to 900°C, along with four endothermic peak at around 75.6 °C, 139.6 °C, 295.2 °C and 798.6 °C. The largest weight loss observed between 88 °C and 190 °C accompanied by an endothermic peak at 139.6 °C was as ascribed to the physical water release from NaOH and MT sample. In this temperature range 4.4 % mass loss was occurred. The endothermic peaks at 295.2 °C, together with the mass loss of about 3.5 %, probably referred to the dehydration of muscovite and sodalite in the MT sample. In the temperature range of 500-1000°C, 2.83% mass loss was observed. The mass loss was believed to be caused by the gradual dissolution of aluminosilicate minerals in MT into melting NaOH.

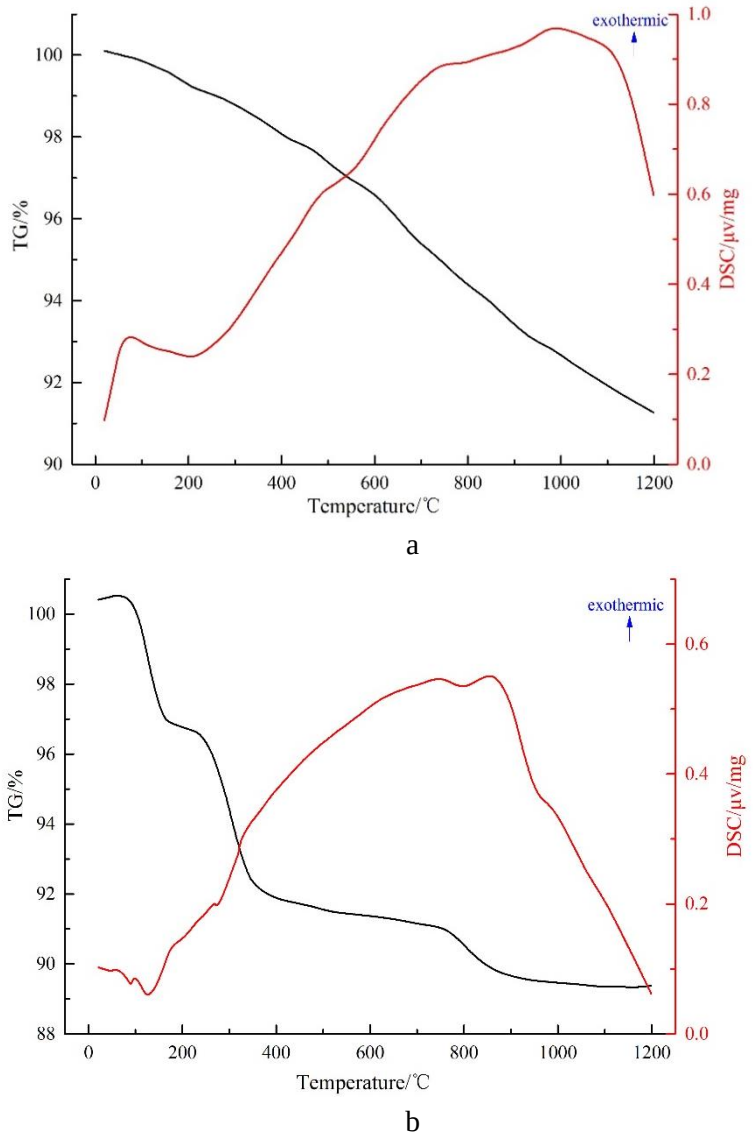

Figure 2. TG-DSC curves of the MT and FMT3 specimen (a=FM; b=FMT3).

FTIR spectra of MT and FMT were presented in Figure 3. In Figure 3, bands at 1618 and 1636 cm^{-1} correspond to the O-H stretching vibration which were attributed to water present in the raw material [39]. The absorption bands attributing to asymmetric stretching vibrations of Si-O-T (T=Si or Al, 900-1200 cm^{-1}), symmetric stretching vibrations of Si-O-T (T=Si or Al, 680-780 cm^{-1}), and bending vibrations of Si-O-T (T=Si or Al, 460–490 cm^{-1}) [40, 41] decreased after alkali fusion treatment. This indicated the decrease of crystalline phases in FMT and the formation of amorphous phases [36] due to the hydrolyzation of Si-O-T (T=Si or Al) bonds with the action of alkali. This could be confirmed by the XRD patterns which showed a broad hump between 20 and 40° (2θ) (Figure 2). The strong band between 1300 and 1550 cm^{-1} were related to stretching vibration of O-C-O group [42], suggesting the presence of carbonate minerals (such as calcite or cancrinite) in MT/FMT samples. However, they were not been identified by XRD analysis (Figure 2) here, which indicated that these minerals were poorly crystallized. Furthermore, as the amount of NaOH increase, the intensity of the band between 1300 and 1550 became more acute. At 550°C, MT were not completely converted into amorphous phases, leaving some unreacted NaOH reacting with the CO_2 from atmosphere [38, 43].

The broad band around 3100 cm^{-1} attributed to O-H stretching and the intensity of this band increased with the increase of NaOH content.

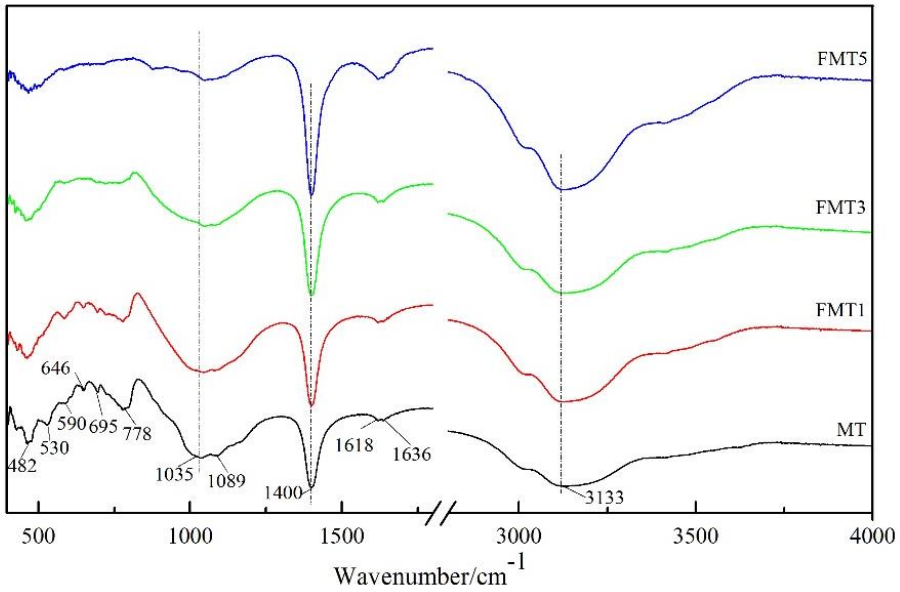

Figure 3. FTIR spectra comparison of MT and FMT.

The testing results of MT/FMT solubility in NaOH solution (10mol/L) were shown in Figure 4. Generally, there was a dramatic increase in the concentration of reactive Si and Al as a function of NaOH content. MT recorded the lowest concentration of reactive Si and Al (0.095 g/L) while FMT5 showed the highest concentration (2.52 g/L). The increase in the concentration of reactive Si and Al suggested that the alkali fusion treatment resulted in the break of some highly crystalline phases and the release of silica and alumina, which could increase the reactivity [36].

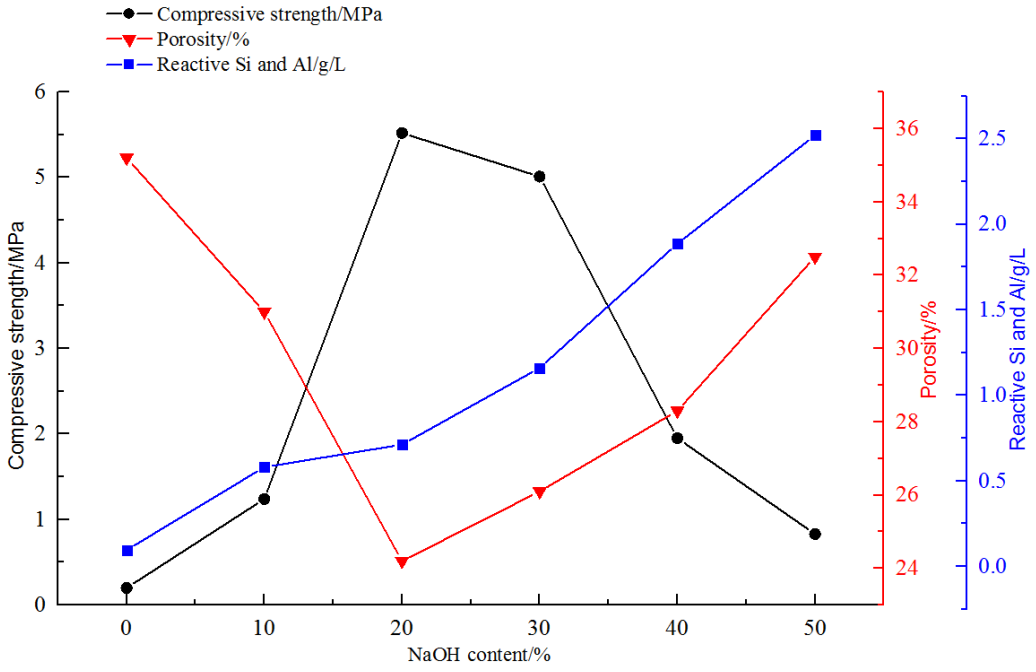

Figure 4. Reactive Si and Al content, compressive strength and porosity.

3.2. Characterization of BFM samples

The compressive strength and porosity of BFM samples as a function of NaOH content was determined at ambient temperature and the results presented in Figure 4. As it was presented in Figure 4, the compressive increased between 0.20 MPa (sample BFM0) and 5.12 MPa (sample BFM2) and then decreased to 0.83 MPa (sample BFM5). The increase in strength in geopolymer mortar was attributed to the increase of reactive Si and Al content (Figure 4). While when the NaOH content exceeded 20%, excess of alkali hindered geopolymerization process although the reactive Si and Al content increased continuously. This may resulted from the increase in the coagulation of silica [44,45]. On the other hand, the excess OH^- concentration would cause aluminosilicate gel precipitation at very early stages [46], which subsequently hindered geopolymerization and led to higher porosity (Figure 4). In a similar study, L.N. Tchadjié [36] reported that the compressive strength of geopolymer increased up to 40%wt of Na_2O used during alkali fusion followed by a decrease. Take strength requirement (0.5-5MPa) and cost of paste backfilling into consideration, FMT2 could be the best choice in this study to be used in mine filling.

SEM micrographs of BFM samples were presented in Figure 5 a-d, which shown heterogeneous texture with many cracks and pores. With the increase of NaOH content to 20%, a reduction of cracks and pores was observed, which resulted from the presence more soluble Si and Al (Figure 4). Through geopolymerization, reactive Si and Al would be transferred into geopolymer gels, acting as filler into cracks and decrease porosity (Figure 4). This would explained the increase of compressive strength of BFM samples. Increasing the NaOH content to 50%, more pores were identified due to the poor geopolymerization.

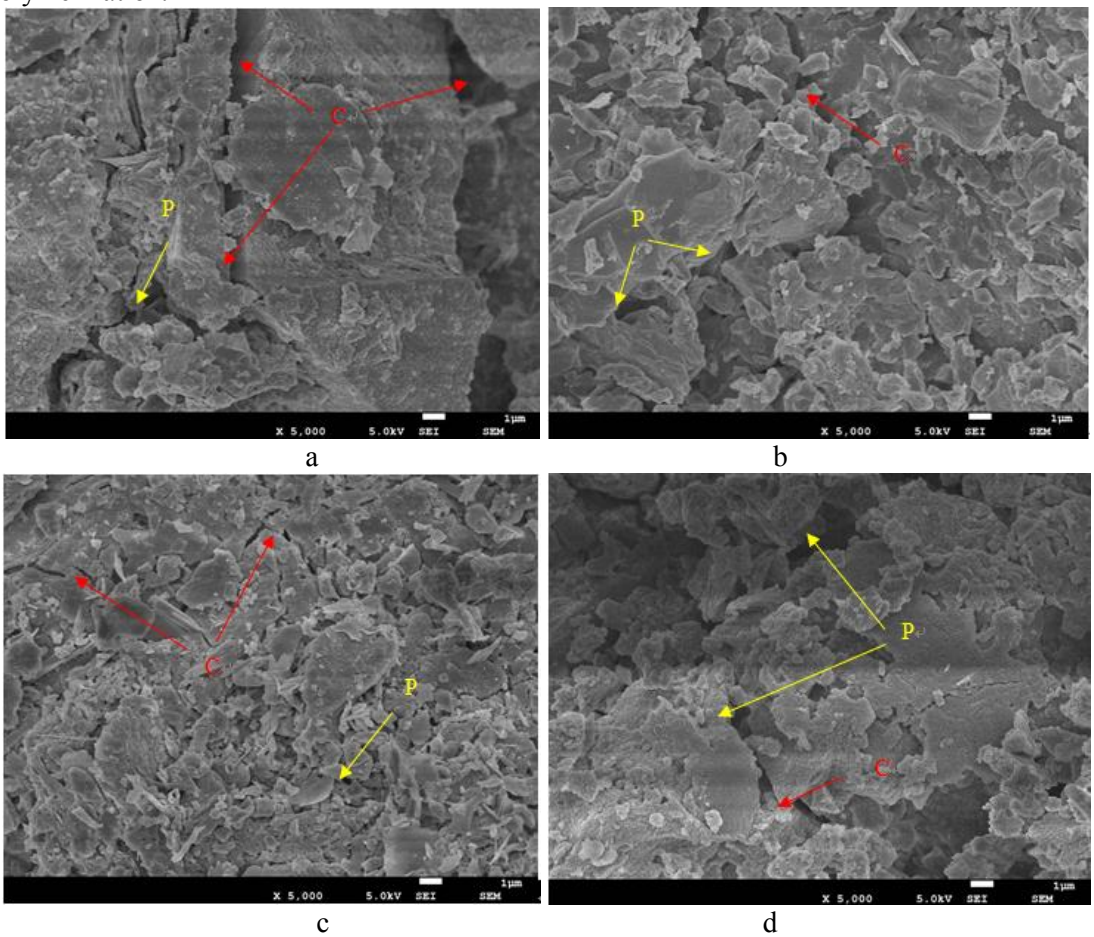

Figure 5. Microstructure of BFM samples: (a=BFM0; b=BFM1; c=BFM2; d=BFM5). (C-Cracks; P-Pores)

4. Conclusions

Raw metal mine tailings shown little geopolymerization ability in NaOH solution. The structure of metal mine tailings broke down through alkali fusion activation with the increasing amount of reactive Si and Al. The compressive strength of metal mine tailings based backfilling materials through geopolymerization increased as a function of NaOH dosage in the process of alkali fusion, but decreased when the NaOH content exceeded 20% due to poor geopolymerization. As a result, synthesis of geopolymer using alkali fusion pretreatment metal mine tailings shown a great potential to be used in backfilling.

Acknowledgements

The authors gratefully acknowledge the financial support from Project(51774066) supported by the National Natural Science Foundation of China and Project (2018YFC0604604) supported by National Keypoint Research and Invention Program of the Thirteenth.

References

[1] Lee J K, Shang J Q and Jeong S 2014 *J Hazard Mater* **276** 323-331
[2] Adiansyah J S, Rosano M, Vink S and Keir G 2015 *Journal of Cleaner Production* **108** 1050-1062
[3] Barrie E et al. 2015 *Applied Clay Science* **109-110** 95-106
[4] Hansen R N 2015 *Applied Geochemistry* **61** 217-223
[5] Rao F and Liu Q 2015 *Mineral Processing and Extractive Metallurgy Review* **36** 399-409
[6] Salinas-Rodríguez E, et al. 2016 *Hydrometallurgy* **160** 6-11
[7] Leiva M A and Morales S 2013 *Ecotoxicol Environ Saf* **90** 167-173
[8] Nejeschlebová L et al. 2015 *Journal of African Earth Sciences* **105** 17-28
[9] Kondrat'eva T F et al. 2012 *Hydrometallurgy* **111-112** 82-86
[10] Bailong L, Zhaohui Z, Linbo L and Yujie W 2013 *Rare Metal Materials and Engineering* **42** 1805- 1809
[11] Yang X, Huang X and Qiu T 2015 *Minerals Engineering* **84** 100-105
[12] Pia G, Casnedi L and Sanna U 2015 *Ceramics International* **41** 6350-6357
[13] Sari Yilmaz M and Piskin S 2015 *J. of the Taiwan Institute of Chemical Engineers* **46** 176-182
[14] Onuaguluchi O and Eren Ö 2016 *Journal of Cleaner Production* **112** 420-429
[15] Yao Y and Sun H 2012 *Fuel* **97** 329-336
[16] Yao Y and Sun H 2012 *J Hazard Mater* **213-214** 71-82
[17] Cihangir F, Ercikdi B, Kesimal A and Turan A 2012 *Minerals Engineering* **30** 33-43
[18] Cihangir F, Ercikdi B, Kesimal A, Deveci H and Erdemir F 2015 *Minerals Engineering* **83** 117-127
[19] Slaty F, Khoury H, Wastiels J and Rahier 2013 *Applied Clay Science* **75-76** 120-125
[20] Ferreira L, Branco F G, Costa H S S,Julio E and Maranha P 2015 *Construction and Building Materials* **95** 337-344
[21] Aredes F G M, Campos T M B, Machado J P B, Sakane K K, Thim G P and Brunelli D D 2015 *Ceramics International* **41** 7302-7311
[22] Nazari A, Khalaj G, Riahi S, Bohlooli H and Kaykha M M 2012 *Ceramics International* **38** 3111-3120
[23] Nazari A, Torgal F P, Cevik A and Sanjayan 2014 *Ceramics International* **40** 6053-6062
[24] Palmero P, Formia A, Antonaci P, Brini S and Tulliani J-M 2015 *Ceramics International* **41** 12967-12979
[25] Ahmari S and Zhang L 2012 *Construction and Building Materials* **29** 323-331
[26] Abdollahnejad Z, Pacheco-Torgal F, Félix T, Tahri W and Barroso Aguiar J 2015 *Construction and Building Materials* **80** 18-30
[27] Al-Harahsheh M S, Al Zboon K, Al-Makhadmeh L, Hararah M and Mahasneh M 2015 *Journal of Environmental Chemical Engineering* **3** 1669-1677

[28] Bernal S A 2015 *Construction and Building Materials* **98** 217-226
[29] Jin F, Gu K and Al-Tabbaa A 2015 *Cement and Concrete Composites* **57** 8-16
[30] Zhang N, Liu X, Sun H, Li L 2011 *Cement and Concrete Research* **41** 270-278
[31] Ahmari S, Zhang L 2013 *Construction and Building Materials* **44** 743-750
[32] Komnitsas K and Zaharaki D 2007 *Minerals Engineering* **20** 1261-1277
[33] Duxson P and Provis J L 2008 *Journal of the American Ceramic Society* **91** 3864-3869
[34] Xu H, Li Q, Shen L, Shen L, Zhang M and Zhai J 2010 *Waste Manag* **30** 57-62
[35] Rieger D et al. 2015 *Construction and Building Materials* **83** 26-33
[36] Tchadjié L N, Djobo J N Y, Ranjbar N, Tchakouté H K, Kenne B B D, Elimbi A, Njopwouo D, 2019 *Ceramics International* **42** 3046-3055
[37] Kouamo Tchakoute H, Elimbi A, Diffo Kenne B B, Mbey J A and Njopwouo D 2013 *Ceramics International* **39** 269-276
[38] Feng D, Provis J L, Deventer J S J and Scherer G 2012 *Journal of the American Ceramic Society* **95** 565-572
[39] Guo Q, Qu J-k, Han B-b, Wei G-y and Zhang P-y 2014 Transactions of Nonferrous Metals Society of China **24** 3979-3986
[40] Ke X, Bernal S A, Ye N, Provis J L, Yang J and Biernacki J 2015 *Journal of the American Ceramic Society* **98** 5-11
[41] Ye N et al. 2014 *Journal of the American Ceramic Society* **97** 1652-1660
[42] Li Q, Xu H, Li F, Li P, Shen L, Zhai J 2012 *Fuel* **97** 366-372
[43] Criado M, Fernández-Jiménez A, Palomo A, Sobrados I and Sanz J 2008 *Microporous and Mesoporous Materials* **109** 525-534
[44] Andini S, Cioffi R, Colangelo F, Grieco T, Montagnaro F and Santoro L 2008 *Waste Manag* **28** 416-423
[45] Görhan G and Kürklü G 2014 *Composites Part B: Engineering* **58** 371-377
[46] Somna K, Jaturapitakkul C, Kajitvichyanukul P and Chindaprasirt P 2011 *Fuel* **90** 2118-2124